Paper presented at Dynamics and Control of Systems and Structures in Space (DCSSS),
6th conference, Riomaggiore, Italy, July 2004

# Numerical Simulation of High Velocity Impacts on Thin Metallic Targets I

Rade Vignjevic, James Campbell, Séverine Lepage
Crashworthiness, Impact and Structural Mechanics (CISM)
Cranfield University, UK

## Abstract

Spacecraft encounter various impact phenomena in space, among which orbital debris impacts are of most concern. These impacts occur at a wide range of velocities. Impact velocities from a few hundreds m/s to one km/s are common in geostationary orbit and even occur in low Earth orbit. However, these high velocity impacts are not fully characterised. It's required to study the shielding performance in order to assess the spacecraft survivability in the event of high velocity impacts.

The paper is divided into two parts. Overall it investigates the capability of hydrocodes to simulate high velocity impacts. Particular interest is given to the post-penetration debris cloud characterisation and the material failure mode identification. Three different methods were used to simulate the impact of an aluminium sphere on a thin aluminium plate. The first part, considers analyses performed using a finite element model with element erosion and a discrete element method where the problem is modelled with discrete finite elements with nodes tied with breakable linkages. The second part of the paper considers the same problems with the Smoothed Particle Hydrodynamics (SPH) method using the MCM solver developed at Cranfield University.

All three methods showed good agreement in terms of target damage with the available experimental results. However, their performances are different in terms of debris cloud and failure mode characterisation. As a large number of elements are deleted, the element erosion method shows problems in the petaling failure mode representation and doesn't allow the post-penetration debris cloud to be characterised. In order to be more reliable, the SPH method needs improvements, in particular to avoid tensile instability. The discrete element method allows good representation and identification of the failure modes even if some improvements in the definition of the node linkage failure criterion are required.

## Introduction

Space debris impacts have been studied for more than 50 years, studies began in 1947 with Whipple [18] who considered the threat from natural meteoroids. More recently attention has shifted to the threat from man-made debris.

The characteristics of debris impacts differs LEO and GEO. The average collision velocity in LEO is higher than in the much higher circular GEO orbits. In GEO, characterised by an orbital velocity around 3km/s and an inclination lower than five degrees, impact velocities range from a few hundreds meters per second to just over one kilometre per second. Even if hypervelocity collisions are dominant in LEO, lower velocity impacts can also occur on the rear side of spacecraft.

Space debris shield can be effective against small particles of up to 1cm in size. Weight effective debris shields against particles larger than 1 cm is not technically feasible. Fragments larger than 10 cm are ground-tracked so that collision probability with spacecraft is known and avoidance manoeuvre can be performed when required. Protection against particles 1-10 cm in size can be achieved through special features in the design of space systems (redundant subsystems, frangible structures, pressure vessel isolation capabilities, maximum physical separation of redundant components and paths of electrical and fluid lines etc.).

The development of effective protection requires a good understanding of impact phenomena. Impacts are investigated by three main approaches: analytical, experimental and numerical. Each of the three procedures has its own merits and disadvantages. Experiments are expensive and can not cover all the conditions that can occur in orbit, e.g., impact velocity above 8 km/s. Analytical methods assume a lot of simplifications and are adequate only for a limited range of cases. Numerical results are limited to a single problem since the entire numerical procedure has to be repeated for any change in input variables.

Strictly empirical models and engineering models have been derived from experimental data. These models typically relate hole diameter to various parameters of the target and projectile [5, 13, 15]; or calculate the minimum wall thickness required to avoid penetration [6,7]. These tools allow effective protection devices to be designed. The first implemented protection device, known as Whipple bumper, consists of a thin wall placed in front of the main structure at a sufficient distance. This sacrificial bumper shocks the projectile and creates a debris cloud of projectile and bumper fragments. Many variants of the Whipple shield have been developed, all based on the same energy dilution principle making them efficient only for hypervelocity impacts (i.e. impact velocity larger than the sound speed of the material). At lower velocity, the projectile just penetrates the protection wall, and makes almost direct impact onto the main wall. These high velocity impacts are not well characterised and the shielding performance must be understood in order to carry out spacecraft survivability calculations.

## Objectives and Methodology

Due to the importance of space debris impacts on spacecraft design, the interest in numerical simulations of impacts is growing. As already mentioned, in GEO and even in LEO, impact velocities that range from a few hundreds meter per second to one kilometre per second are frequent. For this category of impacts, actual shielding systems are inefficient. The characterisation of the post-penetration fragments is important in order to evaluate the survivability of the spacecraft to these impacts. If the properties of the debris cloud moving inside a spacecraft are know, it will be possible to develop lethality curves for internal equipment.

Hence, the aim of this study is to investigate the capability of hydrocodes to simulate high velocity impacts. The objectives can be divided into two main tasks:

- The application of modelling methods that can be adequate for the simulation of the phenomena involved in high velocity impacts to representative test cases.

- The comparison of their effectiveness in the determination of the post-penetration fragment characteristics and in the identification of the material failure modes.

Three different Lagrangian methods were used to simulate impact of an aluminium sphere on an aluminium plate:
- Finite element method with element erosion
- Smooth Particle Hydrodynamics (SPH) method
- Discrete Element Method.

The finite element and discrete element cases were simulated using the commercial hydrocode LS-Dyna (vers.960)[12] was used to simulate the test cases, and are described in this paper.

In order to compare the different modelling techniques, two test cases (see Table 1 for details) were chosen. These problems are taken from Bennetti [3]. They consist in the normal impact of a sphere of 5.5-mm radius on a 3.2 mm thick target. Both the target and the projectile are made of aluminium alloy Al2024-T3. The two problems differ in the impact velocity: 500 m/s and 817 m/s. These two cases were chosen because:
- Some experimental results are available.
- The failure modes are different in the two impact velocities.

| | |
|---|---|
| Projectile diameter | 11 mm |
| Target plate thickness | 3.2 mm |
| Projectile material | Al2024-T3 |
| Target material | Al2024-T3 |

Table 1: Test case principal characteristics [3]

Finally, the results are compared. Particular attention is paid to the prediction of: the hole dimension, target deformation, impact-induced stresses, projectile residual velocity, material failure mode and debris cloud characteristics.

## Impact simulation

The understanding of physics involved in impacts is necessary to carry out good numerical analyses. This work considers high velocity impacts at normal incidence on thin metallic targets. A sphere represents the projectile in accordance with the common practice used in space debris simulation. The target and the projectile are both of the same material.

Whereas effects of shock waves and hydrodynamics behaviour dominate hypervelocity impacts, high velocity impacts are dominated by inertia and material failure; with different types of failure modes of the target depending on the geometry of problem, the impact velocity and obliquity and the material characteristics. Penetration may involve a variety of mechanical processes, either singly or in combination.

For thin targets, dishing is expected, as the work to bend and stretch the plate is less than the work to radially expand a hole. Dishing is bending deformation of the plate

which may extend to considerable distances from the impact area. Failure would begin with bending then the projectile would perforate the target and pass through it completely, inducing plugging and possibly petaling.

Plugging failure occurs when the conditions are such that there is very little radial material flow and the material ahead of the projectile is pushed forward and eventually shears out. Both the bluntness of the projectile and the hardness of the target tend to minimise radial flow. In the shear band plug failure, the perforation is caused by the shear stresses along the shear band in the direction of projectile velocity. The plug diameter is generally less than the projectile dimension due to the initial dishing.

In petaling mode, target failure initiates at a point ahead of the projectile and propagates radially outward along several discrete paths forming several triangular shaped petals that are bent outward away from the penetrator axis as the penetrator perforates the target. This failure is produce by radial and circumferential tensile stresses.

Hydrocodes, are a common tool for simulation of transient large deformations of solids and structures. The nonlinear response of materials and structures is obtained by solving the conservation equations, equation of state and a constitutive model. To solve this set of equations, they are discretised in space and time. A variety of hydrocodes differ only in the spatial description and time integration schemes utilised.

Numerical simulation of hypervelocity debris impacts have been extensively studied numerical simulations, only few publications concern high velocity debris impacts. This paper compares the capability of three Lagrangian methods for high velocity impact simulation:

- Finite element method with element erosion
- Smooth Particle Hydrodynamics (SPH) method
- Discrete element method

Bennetti [3] attempted to simulate high velocity impacts using a Lagrangian finite element model with element erosion. This technique suffered from accuracy problems for the simulation of failure involving petaling and crack propagation.

SPH has already been applied to a large range of impacts. For example, Bashurov [2] studied experimentally and numerically the impacts of steel projectile on aluminium and steel plates in the velocity range from 0.5 to 6.5 km/s. He used a SPH method for the numerical simulations, which showed good agreement with the experiments.

The discrete element method is based on element separation to simulate failure. Some similar approaches have been used in the literature. Ambur [1] and Guangyu [8] have simulated the perforation of thin targets by rigid projectiles. They modelled the target with shell elements whose nodes were linked by breakable bonds. This technique modelled accurately petaling and crack propagation. However, Guangyu [8] noted that the shell target model is only valid for very thin targets.

## Element erosion method

As already mentioned, problems occur when the classical Lagrangian approach is used for the simulation of high velocity impacts. Indeed, element distortions typical of Lagrangian methods cause undesirable effects including small time step size and element inversion. The implementation of an erosion algorithm, which deletes the heavily distorted elements, offers a solution to overcome these problems and allow the calculation to continue.

Erosion algorithms consist of two main parts: the test that decides when an element is eroded and a method to redefine the contact interfaces after element deletion. Element erosion has been widely used for impact simulation in literature. For example, see Hayhurst [10]. Different deletion criteria exist. A commonly used criterion is based on the effective plastic strain, and alternative criteria have also been investigated [4].

As element erosion does not model a physical effect, the major difficulty is to select a pertinent value for the element failure strain. Indeed, if too many elements are deleted, the physics of the model will not be accurately represented Vignjevic [16] proposed a method to define proper erosion features and so improve the confidence in the obtained results. This method consists in adjusting the element failure strain so that the simulation of the impact on a semi-infinite target gives a penetration depth in agreement with the value predicted by empirical equations. This technique is applied in this work.

## Discrete element method

The discrete element approach consists in modelling the target and the projectile by discrete finite elements whose nodes are initially tied together. Breaking these ties allows elements to separate and cracks to propagate without element deletion so that the mass and momentum are conserved.

Ambur [1] and Guangyu [8] used a similar approach for the simulation of penetration of very thin target. Their model used shell elements whose nodes were tied with breakable bonds. The results showed good agreement with both experiments and erosion element simulations. However, Guangyu discussed the use of shell elements to model the target and formulated a preliminary criterion that governs whether a target can be accurately modelled by shell elements. According to this criterion, the test cases studied in this study can not be modelled with shell elements. The technique of tied node with failure will be extended to solid elements. Weemes [17] used this discrete element approach in bird strike simulations. However, this technique showed some deficiencies that the author couldn't solve because of time constraint. The main problems encountered were the contact definition between all the elements and numerical instability of some elements.

In this work nodes were tied using generalised spotwelds. The generalised spotweld algorithm is based on rigid body dynamics. Each weld is defined by a set of nodes that moves rigidly with six degrees of freedom until a failure criterion is reached. Welds could fail when the combination of normal and shear forces across

the spotweld reach defined failure forces [12]. The main advantages of this approach over tied node approach are:

- Failure depends only on the failure forces.
- The generation of the model is simpler.
- The definition of the linkages is less CPU consuming.

## FE Model

Using the symmetry of the problem, only one quarter of the geometry is modelled. The sphere and the plate are discretised by 8-node hexahedron solid elements, using one integration point.

The finite element mesh used is shown in Figure 1. The plate has 12 elements along the thickness to allow sufficient resolution.

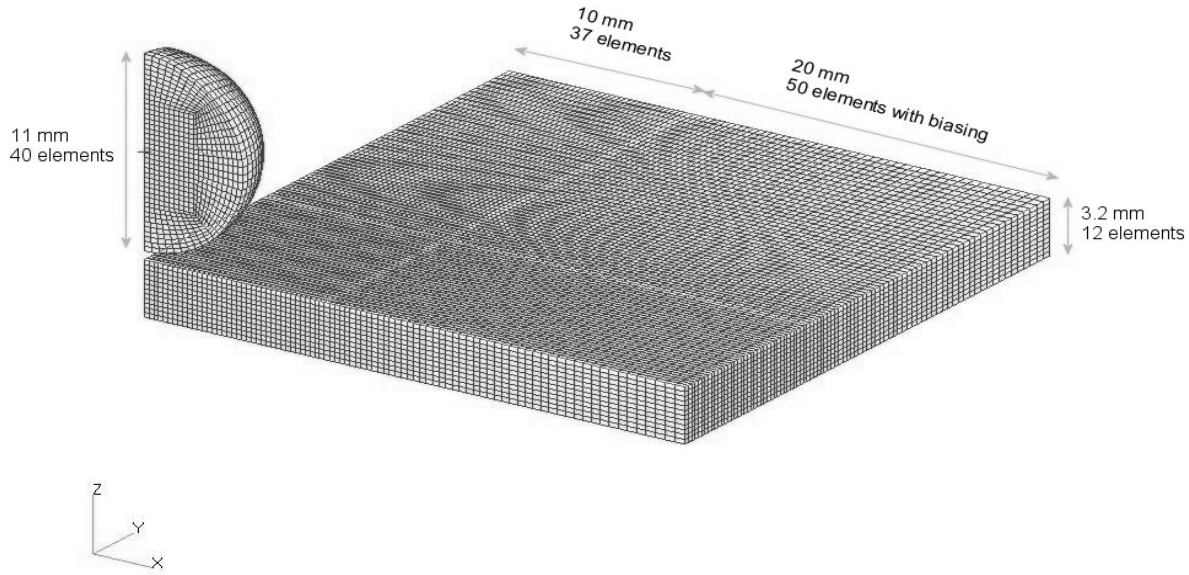



Figure 1: Finite element mesh

The spherical projectile is meshed using a butterfly mesh. The element size is chosen to be similar to that of the impact zone of the plate. The sphere contains 40 elements along its diameter. The butterfly mesh is a better way to model sphere than radial or Cartesian meshes as shown in Figure 1.

### *Material model*

Johnson Cook model was chosen, as it is applicable to most metals and the range of deformations and strain rates of interest. Moreover it includes a damage and a tensile failure model. This material model was used in all simulations in this study. The material parameters are taken from Johnson-Cook [11] and are summarised in Table 2. The Johnson-Cook model requires an equation of state. While the constitutive equation models the deviatoric behaviour, the equation of state models the hydrostatic behaviour. For this study the Grüneisen equation of state is used [9]. The equation of state variables are taken from [3].

| | | | |
|---|---|---|---|
| A [MPa] | 265 | Specific heat [J/kgK] | 875 |
| B [MPa] | 426 | Melting temperature [K] | 775 |
| c [-] | 0.015 | Room temperature [K] | 300 |
| m [-] | 1 | Tensile strength, Ultimate [MPa] | 485 |
| n [-] | 0.34 | Shear modulus [GPa] | 28 |
| Density [kg/m³] | 2 780 | | |

Table 2: Material constants for Al2024-T3 from [11, 14].

***Element erosion model***

The element erosion criterion is based on the effective plastic strain. The element effective plastic strain is compared to the failure strain and once this is reached, the element is deleted. The failure strain is a measure of the maximum allowed deformation of an element before its deletion and it can be expressed as [9]:

$$\varepsilon^f = \left(D_1 + D_2 \exp D_3\sigma^*\right)\left(1 + D_4 \ln \varepsilon^*\right)\left(1 + D_5 T^*\right) \qquad (1)$$

where $D_i, i = 1,...,5$ are input constants and $\sigma^*$ is the ratio of the pressure to the effective stress.

Determination of the *D* parameters is not straightforward as already mentioned. The values of $D_i$ used were determined by Bennetti [3], who used the method proposed by Vignjevic [16]. Indeed, these values give a crater depth $P_\infty$ of 4.97 mm in a semi-infinite target for an impact velocity of 800 m/s. Taking into account the limitation of accuracy introduced by the discretisation, this value is similar to 4.92 mm which is the value predicted by empirical models [6].

The tensile failure model based on the default pressure limit was used. The initial value for the limit pressure was set to the ultimate tensile strength which is 485 MPa for Al2024-T3 [14].

***Discrete element model***

To generate a discrete element mesh, first a standard mesh is generated using standard tools. Then specially developed tools are used to transform the finite element model in a discrete element model: the first step is to duplicate nodes so that every element is independent, then spotwelds are defined between coincident nodes, finally each element is scaled so that the nodes are no more strictly coincident.

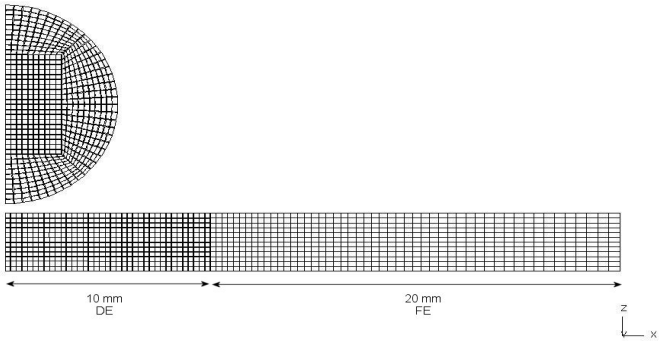



Figure 2: Discrete element model (DE: Discrete Element and FE: Finite Element)

The mesh is the same as in the element erosion model. Discrete elements replace classical finite elements in the projectile and in the plate just under the projectile: a square of 10-mm sides (Figure 2). The element dimensions are scaled by a factor of 90%. Several trials were performed to fix this value, the scale factor was decreased until errors due to spotweld between coincident nodes no more occur during the initialisation of the problem. The inner part of the projectile, which is modelled with discrete elements, is tied to the outer part by a tied-nodes-to-surface-with-offset contact. Symmetry planes are defined by restraining the adequate nodal degrees of freedom. The outer boundaries are fully constrained and a non-reflective boundary condition is applied. All the elements are included in the definition of an automatic eroding single surface contact. The penalty stiffness scale factor is set to 0.7 as in the element erosion model. This value satisfactorily eliminates the problems of interpenetration between the elements and at the interface. The normal and shear failure forces are related to the ultimate tensile strength and the shear strength:

$$F = \frac{A\sigma}{4} \tag{2}$$

where: $F$ is the normal or shear failure force

$A$ is the cross section area of an element

$\sigma$ is the ultimate tensile or shear strength. The quasi-static value is 485 MPa and 283 MPa for respectively, the tensile and shear strength [14].

The largest element dimension is 0.43 mm, so A is set to $0.43^2 = 0.1849$ mm².

In order to avoid an early termination, element erosion has been added to the model the delete the elements. The element strain failure is set to 1.5, this allows a normal termination without deleting too many elements.

A B

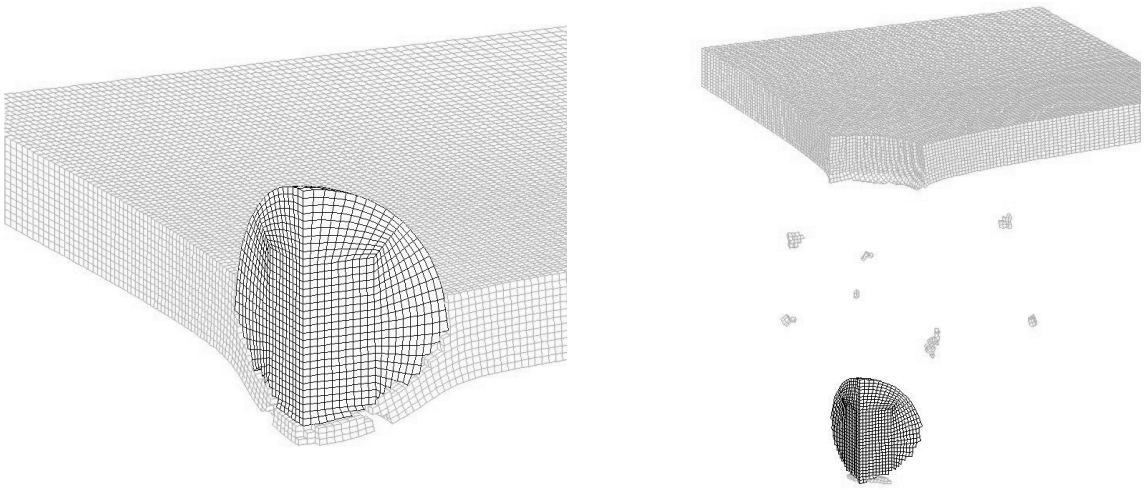


Figure 3: Perforation mechanisms in the erosion model for the impact velocity of 817 m/s. Resulting deformation at 10 μs (A) and 50 μs (B)

## Element Erosion Results

Two impact velocities are considered: 817 m/s and 500 m/s. The size of the hole left in the target, the perforation mechanisms, the mass losses and projectile residual velocity were considered.

### *Impact velocity: 817 m/s*

Figure 3 shows that plugging as well as petaling occurred. Bulging clearly appears in the beginning of the penetration. The rear side of the plate deforms according to the shape of the penetrator. Then, a plug is ejected (Figure 3 A). The hole left in target is smaller than the projectile, hence the lips of the hole are bent as the projectile pushed them. Then, when the tensile strength is exceeded, cracks should begin to develop around the hole and form petals. However, all the elements that should form these petals were deleted and no crack propagation was simulated. This shows the limit of the element erosion based approach for crack propagation and especially petaling simulation. Moreover, at the end of the penetration, most of the element that should constitute the debris cloud were deleted, see Figure 3 B.

The hole left in the plate had a radius of 5.55 mm. This is measured on the upper side of the target. The height of the projectile has been reduced from 11 mm to 8.61 mm. The plate experiences a mass loss of 2.16 % and for the projectile, it's 28.5 %. One consequence of this mass erosion is the decrease of the total energy (Figure 6).

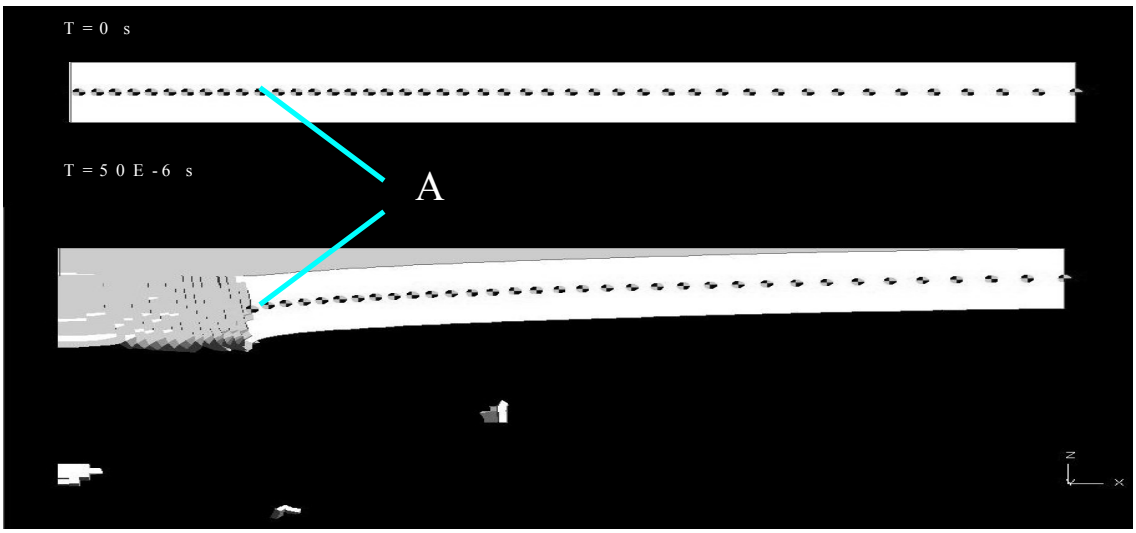



Figure 4: Target bending. The markers indicate the nodes for which the z-displacement is plotted in Figure 8.

The target also experiences dishing. The bending of the plate is illustrates in Figure 4. This bending can be quantified by the nodal z-displacements of the neutral plane. The displacement of the node A situated at the edge of the hole reaches 1.64 mm at the end of the simulation. It should be noted that the plate deformation is still evolving at 50 µs. Figure 5 shows that 17 µs after the impact, the projectile stops slowing down and its residual velocity is 607 m/s. At this time, there is no more interaction between the projectile and the target.

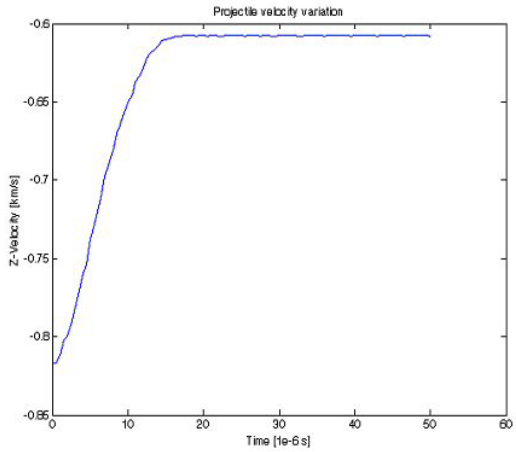



Figure 5: Projectile Z-velocity vs. time

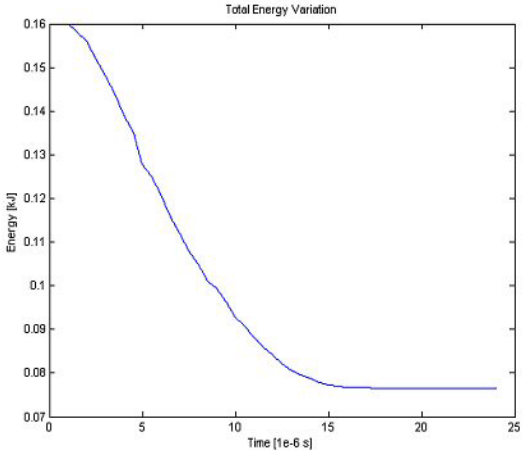



Figure 6: Total energy vs. time

***Impact velocity: 500 m/s***

Figure 7 shows that the dominant failure mode was plugging. The plug ejected by the projectile separated from the projectile due to the release of the elastic stresses in the penetrator-plug assembly. Petaling was also present as some remains of petals are on the rear face of the plate. Compared with the previous case, more information is available about the debris cloud.

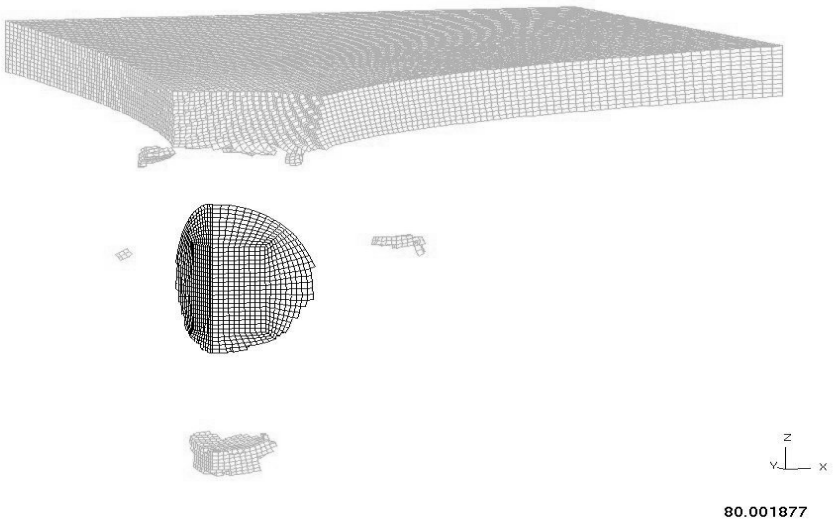



Figure 7: Resulting deformation at time 80 μs for the impact velocity of 500 m/s.

The hole left in the plate has a radius of 5.73 mm. The final height of the projectile is 9.43 mm. Both the plate and the projectile have loss mass due to element erosion. The projectile has suffered a mass loss of 20.6 %. The mass of the target has been reduced by 2.10 %. The mass loss is less important in this case than in the previous one, where the impact velocity was higher. Indeed, all the elements that should form the petals were deleted in the 817m/s impact and here the elements of the plug are not deleted. The height of the projectile is less reduced in this case than in the previous one. (9.43 mm > 8.61 mm)

During the impact process, the plate is also bent. The dishing is more important in this case than in the previous one. The maximum Z-displacement, 3.11 mm, occurs at time 65 $\mu s$ at the edge of the hole. The projectile is slow down during the impact. The evolution of the z-component of projectile velocity is recorded. 40 μs after the impact, the velocity becomes constant at 208 m/s.

## Discrete Element Results

### *Impact velocity: 817 m/s*

Three different cases were considered:

- Only tensile failure is allowed. (Figure 8, LHS)In this case, no spotweld fails. The failure occurs by element deletion, which had been introduced to delete the unstable elements and not to simulate failure.
- Both tensile and shear failures are allowed. (Figure 8, Centre) A nearly circular plug is formed and cracks propagate radially.
- Only shear failure is allowed (Figure 8, RHS). Only the failure creating the plug is present. There are no radial cracks.

The comparison of these three cases allow us to clearly identify the failure modes. Firstly, a plug is ejected as a result of shear bands. Then, as the projectile pushes further the lips of the hole left after plugging, tensile stress develops, cracks propagate and petals are formed. This is an under-developed petaling mode. Figure 9 (LHS) also shows the presence of these two modes.

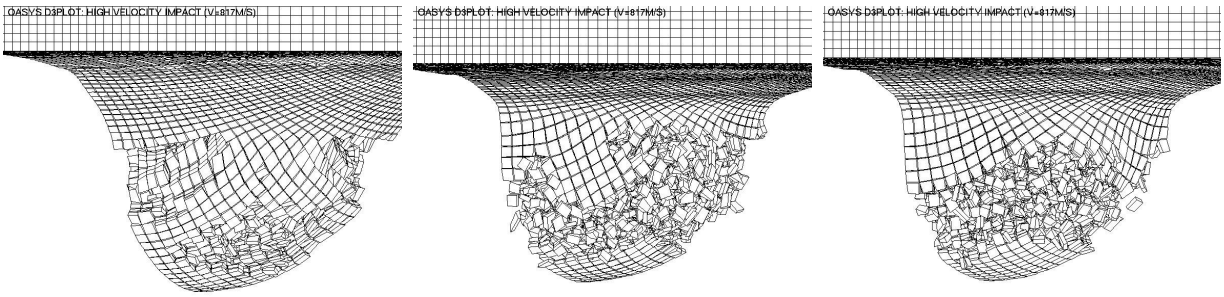



Figure 8: Rear side of the target at time 18 μs when allowed failure is: only normal (LHS), normal and shear (Centre), only shear (RHS)

Because of the discretisation, the failure is not sharply located. Several elements separate to generate failure. These isolated elements perturbed the debris cloud evolution. Figure 9 (RHS) shows the configuration at time 50 μs. Even if a large number of elements are isolated, a set of element forms a plug under the projectile. Moreover at 22 μs, the penetration process can be considered to be finished as the projectile velocity no more evolves (Figure 10). The configuration at 22 μs (Figure 9, LHS) provides enough data to study the threat posed by of the debris cloud or to develop lethality curves.

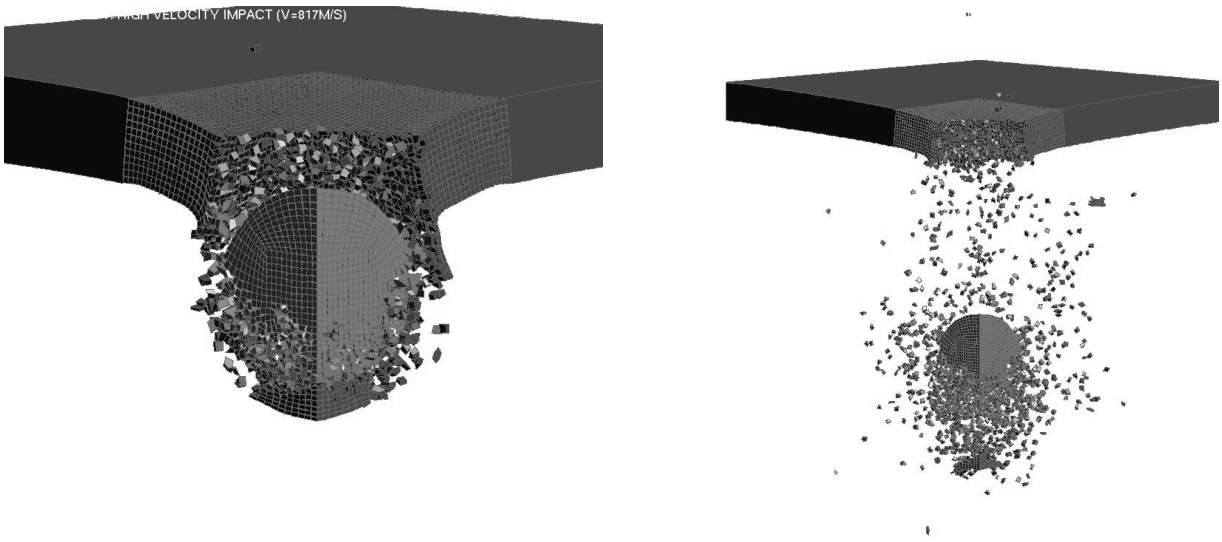



Figure 9: Target and projectile deformation at time 22 μs (LHS) and 50 μs (RHS)

The plate experiences dishing that can be quantified by the displacement of nodes situated on the neutral plane. At the end of the simulation, the displacement of a point on the edge of the hole is 2 mm.

The hole radius, measured on upper face, is 5.4 mm. The projectile height at time 22 μs is 7.7 mm. The impact-induced z-stress is 4.4 GPa and 4.2 GPa in the projectile and target respectively. The projectile velocity decreases from 817 m/s to 500 m/s.

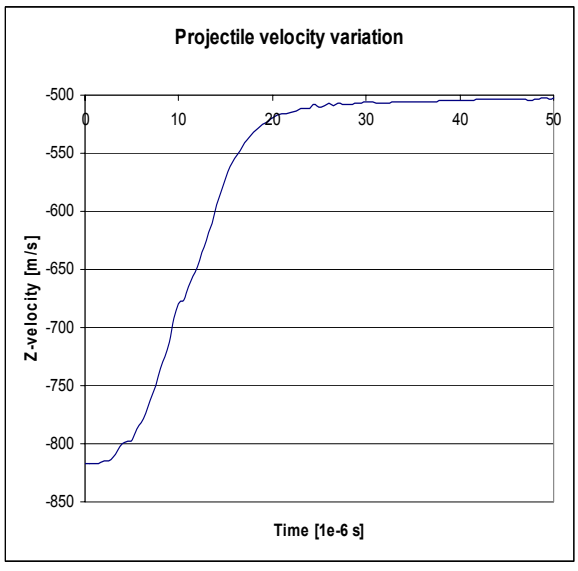



Figure 10: Projectile velocity variation

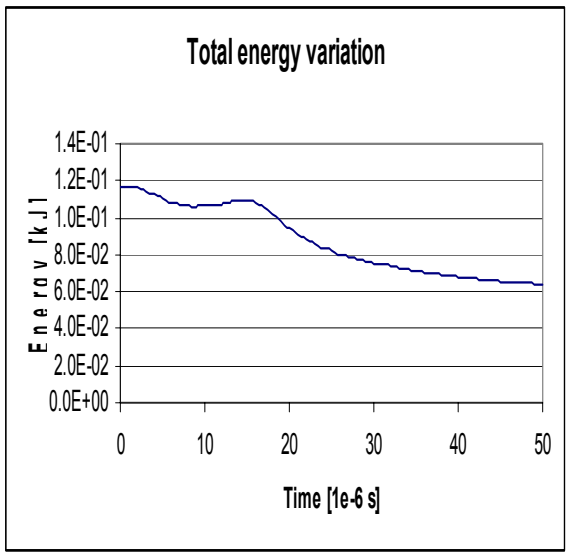



Figure 11: Total energy variation

Figure 11 shows the total energy variation. The energy remains nearly constant during 18 μs. Then the total energy drops because of the element deletion. Hence, the element erosion is used to delete the separated elements that become unstable.

***Impact velocity: 500 m/s***

In this case, the dominant mode of failure is plugging. In Figure 12, the plug, which is separated from the projectile, can be observed. Due to the discretisation, the shear bands were not sharply defined and several elements were separated. This effects the debris cloud. The plate dishing is more important in this case than in the previous one, with a maximum z-displacement of 3.53 mm. The hole radius measured on the upper face is 5.7 mm. The projectile height is 8.4 mm after perforation. The projectile velocity decreases from 500 m/s to 180 m/s in 40 μs.

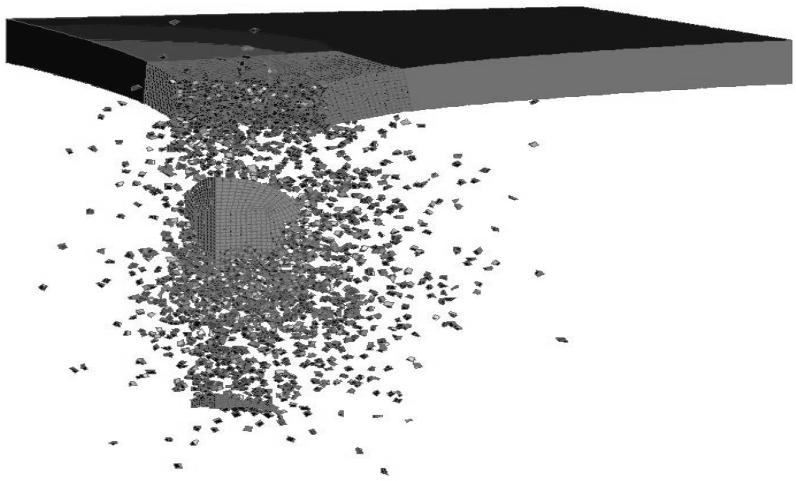


Figure 12: Configuration at time 80 μs, for 500 m/s case.

## Summary

In this study, the capability of hydrocodes in modelling of high velocity impacts has been demonstrated and investigated. High velocity impact test cases were simulated using three different Lagrangian methods: Finite element with erosion, the Smooth Particle Hydrodynamics (SPH) method and the Discrete element method.

These methods were applied to the simulation of the impact of an 11-mm diameter sphere on a 3.2-mm thick plate. Both the target and the projectile were made of Al2024-T3. Two impact velocities were investigated: 500 m/s and 817 m/s. The simulations provided results in terms of failure mechanisms, hole dimension, residual projectile velocity, projectile and target deformation.

This paper presents the finite element with erosion and the discrete element cases. Part 2 of this study presents the SPH results and a detailed comparison of the results for the three methods.

## References

[1] Ambur, D. R. et al, Numerical simulations for high-energy impact of thin plates, *International Journal of Impact Engineering*, Vol. 25, pp. 683-702, 2001.

[2] Bashurov, V. V. et al., Experimental modelling and numerical simulation of high- and hypervelocity space debris impact to spacecraft shield protection, *International Journal of Impact Engineering*, Vol. 20, pp. 69-78, 1977.
[3] Bennetti, A., Numerical and experimental investigation of high velocity impacts for spacecraft protection, MSc Thesis, Cranfield University, 2002.
[4] Campbell, J. and Vignjevic, R., Development of Lagrangian hydrocode modelling for debris impact damage prediction, *International Journal of Impact Engineering*, Vol. 20, pp. 143-152, 1997.
[5] Carey, W.C., McDonnell, J.A.M. and Dixon, D.G., Capture cells: decoding the impacting projectile parameters, *Lunar and Planetary Science Conference XVIth*, Abstracts, 1985
[6] Christiansen, E., Design performance equation for advanced meteoroid and debris shield, *International Journal of Impact Engineering*, Vol. 14. 145-156, 1990.
[7] Cour-Palais, B.G., Hypervelocity impacts in metals, *International Journal of Impact Engineering*, Vol. 5, pp. 221-238, 1987.
[8] Guangyu, S. Junyan, G and Chun, L., Efficient modeling of panel-like targets in perforation simulation, *Third European LS-Dyna User Conference*, Paris, 2001.
[9] Hallquist, J. O., LS-DYNA Theoretical Manual, Livermore Software Technology Corporation, 1998.
[10] Hayhurst, C.J., Ranson, J.H., Gardner, D.J. and Birnbaum, N.K., Modelling of microparticle hypervelocity oblique impacts on thick targets, *International Journal of Impact Engineering*, Vol. 17, pp. 375-386, 1995.
[11] Johnson, G.R. and Cook, W.K., A constitutive model and data for metals subjected to large strains, high strain rates and high temperatures*, Proceedings of 7th International Symposium Ballistics*, The Hague, The Netherlands, pp. 541-548, 1983.
[12] LSTC, LS-Dyna: Keyword user's manual. Volume 1, Version 960, March, 2001.
[13] Maiden, C.J. and McMillan, A.R., An investigation of the protection afforded a spacecraft by a thin shield., *AIAA*, 2(11), 1992-1998, 1964.
[14] Matweb.com, The Online Materials Database. http://www.matweb.com Accessed in July 2003.
[15] Nysmith, C.R. and Denardo, B.P., Experimental investigations of the momentum transfer associated with impact into thin aluminum targets, NASA TN D-5492. October, 1969.
[16] Vignjevic, R., Hughes, K. and Taylor E.A., Finite element modelling of failure of a multi-material target due to high velocity space debris impacts, *Space Debris*, Vol. 2, pp. 41-50, 2002.
[17] Weemes, R., Birdstrike on a sharp edge, Cranfield College of Aeronautics, MSc Thesis, 2001.
[18] Whipple, F.L., Meteorites and Space Travel, *The Astronomical Journal*, vol. 52, 1947.



https://dspace.org/

# Numerical simulation of high velocity impacts on thin metallic targets I and II

**Vignjevic, Rade; Campbell, James C.; Lepage, Séverine**

**2004-12-18T00:00:00Z**
http://dspace.lib.cranfield.ac.uk/handle/1826/790

Downloaded from a DSpace repository. https://dspace.org/